




A Transformational Framework for Analysis of Phase Noise in LC Oscillators

SUDIPTA SAHA , SHOBA KRISHNAN  (Member, IEEE), AND ALLEN A. SWEET  (Life Member, IEEE)
(Regular Paper)

Department of Electrical and Computer Engineering, Santa Clara University, Santa Clara, CA 95053 USA

CORRESPONDING AUTHOR: Sudipta Saha (e-mail: ssaha2@scu.edu).

ABSTRACT Phase noise has become the single most critical factor to be addressed in the design of modern communication systems. Facing the challenging requirements of 5G cellular communication, our paper describes a new theoretical framework to calculate the phase noise of LC oscillators, relying on easy to implement closed form solutions for phase noise calculations. Using closed form phase noise solutions enables oscillator designers to easily implement multiple phase noise calculation options for a number of oscillator circuits, which would be very difficult to implement with the existing mathematically complex phase noise theories. The analytic methods of our theory rely on modeling all real oscillators as having non-ideal or latent behaviors in addition to their primary nature for generating a carrier wave operating at a single frequency with a single amplitude. It is a cascade of these non-ideal transformation processes that produce non-ideal oscillator outputs containing the phase noise sidebands. Enhanced qualitative and quantitative insights into oscillator phase noise performances are achieved by using this approach. We validate our methods by comparing their results with phase noise simulations carried out for a sample CMOS LC voltage-controlled oscillator in 90 nm RFCMOS process using SpectreRF simulator. The results for the oscillator's output $1/f^2$ thermal phase noise, $1/f$ noise upconversion into $1/f^3$ phase noise and the $1/f^3$ corner frequency of phase noise spectrum using our theory yields -136 dBc/Hz at 10 MHz offset, -21.3 dBc/Hz at 1 kHz offset and 2.6 MHz respectively. The corresponding values obtained with SpectreRF simulation are -135.9 dBc/Hz, -23.4 dBc/Hz and 2.1 MHz. The carrier frequency is 5.4 GHz with output power of 9.78 dBm.

INDEX TERMS Amplitude modulation (AM), frequency modulation (FM), flicker noise, injection locking, noise factor, oscillator, phase modulation (PM), phase noise, small signal FM spectrum, thermal noise.

I. INTRODUCTION

Oscillators are ubiquitous in electronic systems. In radio frequency (RF) communication systems they are used for frequency translation of information bearing signals and for channel selection. Also, voltage-controlled oscillators (VCO) are an integral part of a phase locked loop (PLL) which by itself serves as a core frequency reference.

Oscillators are susceptible to noise. Noise injected into an oscillator by its constituent devices or by external means may influence both the frequency and the amplitude of the output signal. In most cases, the disturbance in the amplitude is negligible and only the random deviation in frequency is considered. The latter can also be viewed as a random variation in

the period or a deviation in the zero crossing points from their ideal position along the time axis.

Phase noise is the frequency-domain representation of these random fluctuations in the phase of the waveform, corresponding to time-domain deviations from perfect periodicity. A perfect oscillator would have only localized output spectral components occurring at discrete harmonic frequencies but in reality, the corrupting noise spreads out these perfect tones, resulting in noise power occupying at neighboring frequencies. This phenomenon is known as phase noise and is defined as the ratio of the noise power in a 1 Hz bandwidth, at some frequency offset from the carrier, to the power in the carrier [1], [2]. Fig. 1 shows the power spectrum of an

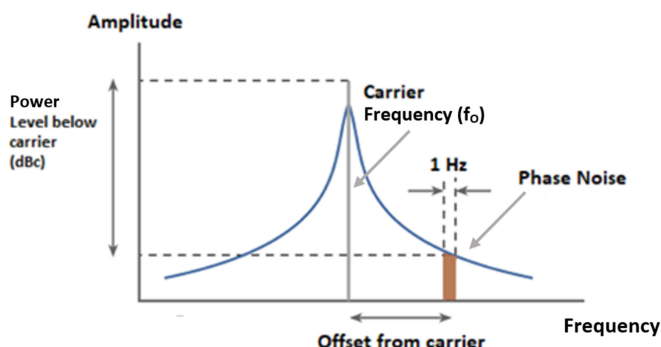


FIGURE 1. Specification of phase noise.

oscillator with upper and lower noise sidebands extending above and below the carrier frequency.

To meet the most ambitious 5G goals, including peak data rates of 10 Gbps, mm Wave frequency bands above 20 GHz are needed. The latest 5G telecommunications technologies demand that significant reductions be made in oscillator phase noise to increase their system's data rates by at least an order of magnitude [3], [4]. Today designers need to have detailed physical insight into the root causes of phase noise in order to meet such stringent specifications.

Considerable effort has been expended over the years to develop and understand the phase noise models for LC oscillators [5]–[11]. Previous approaches may be broadly classified as circuit-based models [12]–[16] and mathematical equation-based models [17]–[25].

This paper describes a new theoretical concept for calculating the phase noise of LC oscillators as closed-form design equations. This circuit-based theory is built on the understanding that phase noise is the direct result of an oscillator's latent non-ideal nature and its own inevitable self-supplied noise inputs that accompany each component's non-ideal nature. The theory evaluates oscillator response to two sources of noise generated on the die itself, thermal noise and $1/f$ noise occurring within the various transistors where the phase of the injected noise is continuously changing in a random fashion. Responses due to external stimulus where the injection source is a coherent signal with a well-known value of phase as a function of time is not considered as part of this work.

Our theory computes $1/f^2$ thermal phase noise, $1/f^3$ close-in phase noise and the $1/f^3$ corner frequency of phase noise spectrum from closed-form equations. It properly addresses the upconversion of baseband flicker noise to $1/f^3$ phase noise at small offset frequencies. Our theory has the ability to provide insight on upper/lower sideband imbalance, when under special circuit conditions, the amplitude modulation (AM) sideband power becomes equal to that of the frequency modulation (FM) sideband power.

Almost all other numerically precise equation-based phase noise models go through a highly mathematical and complicated lengthy process of deriving the phase modulated noise time domain relationships. These models only convert these

relationships into a noise to carrier ratio (N/C) at the end of this long and difficult process. Little intuitive insight into circuit behaviors is offered by these approaches. Our computational flow greatly simplifies this process. Its transformational processes make use of naturally occurring latent circuit behaviors which are ever present in all non-ideal oscillator circuits (i.e., modulation, mixing, injection locking, small signal FM spectral power ratio) that ultimately transform, by naturally occurring circuit processes, the oscillator's internal noise sources into a phase noise to carrier ratio.

Our paper accurately identifies and calculates the sources of phase noise and helps to reduce the complexity of understanding phase noise.

This paper is organized as follows. Section II gives a brief review of previous works on phase noise models and in Section III we develop the Transformational Phase Noise (TPN) theory for qualitative analysis. Section IV develops quantitative analysis to arrive at closed-form expressions for phase noise. Section V validates the TPN computational algorithm by calculating the phase noise of a CMOS LC voltage-controlled oscillator topology using this method and comparing it to the phase noise analysis of the same circuit using the Cadence SpectreRF simulator working with a 90 nm RFCMOS process technology. Finally, Section VI concludes this work.

II. EXISTING PHASE NOISE MODELS

Within the circuit-based model domain field the most well-known phase noise model is Leeson's model that was proposed by D.B. Leeson in 1966 [12]. Leeson proposed an equation for estimating an oscillator's phase noise based on major oscillator parameters – the power of the carrier signal, the quality factor of the resonator and the noise contributions from the active devices. However, no guidelines were given on how to determine analytically the noise contributions of the passive and active components of the circuit or the $1/f^3$ corner frequency. Both of these areas are treated as empirical curve fitting parameters and must be determined from measurements.

Another popular circuit-based linear time invariant model was proposed by Rael, Murphy & Abidi [13], [14] and is based on the decomposition of different noise sources into AM and PM components represented as small rotating phasors superimposed on the main oscillator phasor. However, this model is unable to capture several important effects including the experimental observations of the upconversion of low frequency $1/f$ noise and interactions between amplitude noise and phase noise.

A more accurate linear time variant model was developed by A. Hajimiri and T.H. Lee in 1998 [15], [16]. This model is based on a combination of circuit-based and mathematical equation-based approaches. Its phase noise analysis is based on a conjecture of decomposing perturbations into two (orthogonal) components and generating purely phase and amplitude deviations. This theory introduces the concept of an impulse sensitivity function (ISF) to consider the time

variance and the cyclostationarity effects of phase noise. The model is applicable to all classes of oscillators.

Unlike the approach in [12]–[14], the model in [15], [16] incorporates the time varying nature of an oscillator and can be extended to address the impact of operating nonlinearities within the oscillator loop. However, this approach requires a priori knowledge of the ISF which is usually obtained only through detailed numerical simulations, and straight forward analytical formulations are only available for the simplest oscillator topologies.

From the intuitive concept of ISF, a phase-domain mathematical-equation based macromodel has been developed by Maffezzoni [17]–[19]. This model is able to capture injection locking phenomenon where the oscillator is said to be locked or synchronized to a weak external signal. Maffezzoni proposed a nonlinear time variant phase-domain model based on a perturbation projection vector (PPV). The limitation of this model is that it can only determine the oscillator's response to weak injected harmonic perturbation.

A very rigorous and fundamental approach has been taken by Mirzaei and Abidi [20], [21] for defining the relation between injection locking and phase noise. The work in [21] calculates the Lorentzian spectrum of a free-running LC oscillator arising from the random pulling of its frequency by circuit noise sources.

The most universal and most accurate phase noise model has been proposed by Demir and Roychowdhury [22]–[24] and is based on the PPV concept. It is a mathematically rigorous theory describing the oscillator's phase response to a perturbation using a compact, scalar, nonlinear ordinary differential equation. The main difficulty of this mathematically rigorous model is that it does not provide the circuit designer with any physical insight into the root causes of the phase noise generation mechanisms.

III. TRANSFORMATIONAL PHASE NOISE THEORY QUALITATIVE ANALYSIS

In this section we develop the transformational phase noise (TPN) theory based on qualitative noise analysis of the oscillator. The proposed analytic method relies on an understanding that oscillators have undesired secondary (or latent) roles in addition to their primary role of generating a carrier wave at a single frequency with a single amplitude. These non-ideal natures exhibit their effects by functioning as amplitude modulators (AM), frequency modulators (FM) or an injection locking system responding to internal random noise inputs. In addition to the necessity of considering these latent roles, it is also essential to include as part of the phase noise analysis that oscillators contain internally generated noise sources such as thermal agitation and $1/f$ noise currents which are generated within various circuit components. It is these latent secondary natures of the oscillator that transform its self-generated noise sources through a cascade of transformations to ultimately determine an oscillator's phase noise properties. We present a design-oriented computational procedure that captures how

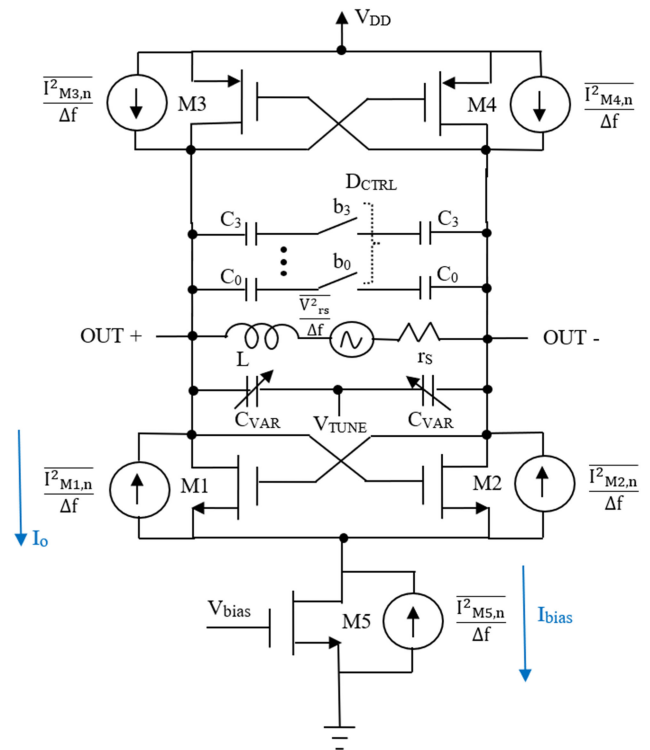


FIGURE 2. Generic CMOS cross-coupled LC voltage-controlled oscillator (VCO) with noise sources.

this transformational derivation is based on a cascade of latent functions, like modulation sensitivities, injection locking bandwidth and small-signal narrowband FM power spectrum calculations leading to the determination of the phase noise.

The accuracy of the proposed TPN theory is validated by calculating the phase noise spectrum of a CMOS LC tank voltage-controlled oscillator (VCO) topology biased by the tail current which is shown in Fig. 2. The thermal current noise density due to the active devices and the voltage noise density due to passive devices are shown.

A. THERMALLY INDUCED PHASE NOISE

Fig. 3 shows the cascade of transformations that are used to calculate the thermal noise contribution to the phase noise spectrum. The initial task is to convert the oscillator's macroscopic temperature into a thermal noise average power density in a 1 Hz bandwidth called the power spectral density (PSD) originating from each source within the circuit in V^2/Hz using circuit parameters from simulation. Here, f_0 is the oscillator's free running carrier frequency, f_M is the noise sideband's offset frequency from the carrier and P_0 is the oscillator's carrier output power. Since ICs are physically small and silicon has high thermal conductivity, we assume the IC die has a single uniform temperature making the calculations inherently macroscopic.

Step 1 is to transform the total PSD of thermal noise sources into random frequency deviation of the carrier by using the

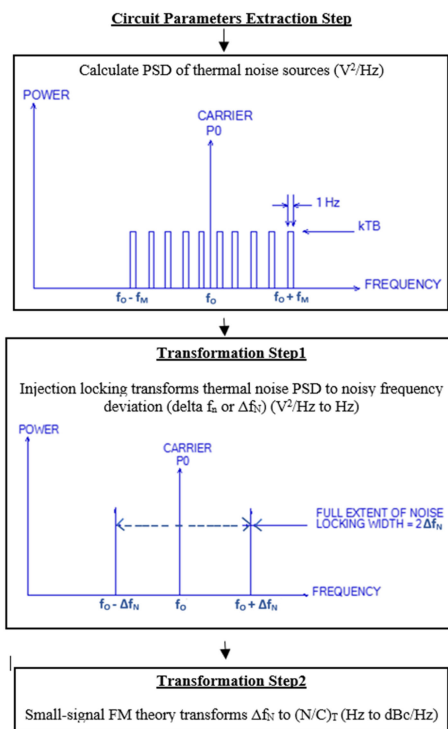


FIGURE 3. LC VCO thermal phase noise transformational flow.

Adler locking equation [26]. Electrical oscillators are sensitive to charge variations. Noise peaks injected instantaneously cause the oscillator’s carrier frequency to suddenly shift back and forth across the carrier frequency as the oscillator tries to “lock” onto the noise power, resulting in a frequency deviation (Δf_N) of the output signal. The transformation units are V^2/Hz to Hz. Step 2 is to transform this frequency deviation Δf_N into a single-sideband noise-to-carrier ratio $(N/C)_T$ using small-signal FM spectral power equation [27]. This transformation is done within the bounds of small-signal FM theory by recognizing that any frequency deviation due to noise injection is inherently small signal. The transformation units are Hz to dBc/Hz.

B. FLICKER NOISE UPCONVERSION INTO A $1/f^3$ PHASE NOISE SPECTRUM

This section presents methods of calculating, using closed form solutions, $1/f^3$ phase noise spectra for LC oscillators. Our methods of phase noise analysis depend critically on recognizing the existence of, and using certain latent characteristics of an ideal oscillator behavior. For instance, an LC oscillator may also create latent AM or FM modulator behaviors. It is this particular latent oscillator behavior that makes possible the upconversion of $1/f$ base band noise into $1/f^3$ phase noise occurring around the carrier frequency.

This section describes the cascade of transformations that are used to calculate the $1/f$ noise current contribution to the $1/f^3$ phase noise spectrum. The $1/f$ noise sources are inherently microscopic and TPN theory considers them as such.

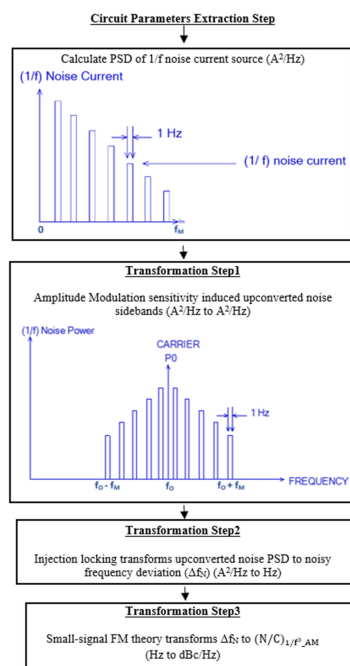


FIGURE 4. LC VCO AM induced $1/f^3$ phase noise transformational flow.

The theory requires one to choose a particular transistor of choice as the source of $1/f$ noise. In this paper we have chosen the tail-bias transistor M5 in Fig. 2 to be the dominant contributor to the $1/f^3$ phase noise spectrum of the LC VCO.

The TPN theory of upconverting the $1/f$ noise into $1/f^3$ phase noise starts with calculating the PSD of the tail-bias $1/f$ noise current in A^2/Hz using circuit parameters from simulation.

1) OSCILLATOR OPERATING AS AM BLOCK

The VCO is functioning as a mixing block whose input is being driven by a modulating signal of frequency f_M in the form of $1/f$ baseband noise current flowing in the tail transistor M5. Here, f_M is the low base band frequency associated with the $1/f$ noise and is also the frequency offset from the carrier frequency of the power spectrum. This modulating noisy signal is naturally created by trapping states that exist within the semiconductor material of the oscillator’s transistors [1], [2].

The mechanism of the upconversion of $1/f$ noise into $1/f^3$ phase noise is due to large-signal commutating mixer action that has been studied extensively [28], [29]. We have used this principle but have analyzed the $1/f^3$ phase noise using our new approach. This non-ideal response upconverts low frequency bias noise and results in the generation of two AM noise sidebands which lie symmetrically about the carrier frequency at $(f_0 - f_M)$ and $(f_0 + f_M)$. This upconverted noise modulates the varactor which modifies the stability of the free running frequency to become phase noise.

Fig. 4 shows the cascade of transformations that are used to calculate the AM induced $1/f^3$ phase noise spectrum. Step 1 is to transform the low frequency tail-bias $1/f$ noise current

PSD in A^2/Hz into AM power sidebands about the carrier frequency in a 1 Hz bandwidth. This is accomplished by using an AM modulation sensitivity obtained from simulation. The transformation units are A^2/Hz to A^2/Hz . Step 2 is to transform the upconverted noise sideband powers into a random frequency deviation of the carrier frequency by using the Adler locking equation [26]. The transformation units are A^2/Hz to Hz. The final step 3 is to transform the noisy frequency deviation Δf_N into a single-sideband noise-to-carrier ratio $(N/C)_{1/f^3_AM}$ by using the small-signal FM spectral power equation. This transformation is done within bounds of small-signal FM theory by recognizing that any noisy frequency deviation is inherently small signal. The transformation units are Hz to dBc/Hz.

2) OSCILLATOR OPERATING AS FM BLOCK

The VCO acting in its unintended role as a FM modulator can also produce random frequency deviation. Similar to a mixer under large signal operation, the cross-coupled pair upconverts the tail noise current into higher-order current harmonics injected into the LC tank. The amplitude of the current harmonics is a function of the bias current in the oscillator. Hence, a change in the bias current caused by $1/f$ noise current injection will result in a shift of the oscillator's frequency [30], [31]. This transformation process in TPN theory is done within the bounds of narrowband FM theory. This resembles the spectrum of the AM case except that in narrowband FM, the phase of the lower sideband is reversed.

Fig. 5 shows the cascade of transformations that are used to calculate the FM induced $1/f^3$ phase noise spectrum. Step 1 is to transform the low frequency tail-bias $1/f$ noise current PSD in A^2/Hz into a random frequency deviated narrowband FM noise sideband spectrum lying about the carrier frequency. This is accomplished by using the FM modulation sensitivity which are obtained from simulation. The FM process by itself produces a frequency deviation and hence the Adler's injection equation is not needed in this case. The transformation units are A^2/Hz to Hz. Step 2 is to transform the noisy frequency deviation Δf_N into single-sideband noise-to-carrier ratio $(N/C)_{1/f^3_FM}$ by using the small-signal FM spectral power equation. The transformation units are Hz to dBc/Hz.

IV. TRANSFORMATIONAL PHASE NOISE THEORY QUANTITATIVE ANALYSIS

In this section we quantify the TPN theory through the cascade of the transformational blocks as discussed in Section III. We arrive at sets of closed-form equations for the thermal phase noise (Section A), $1/f^3$ phase noise (Section B & C) and $1/f^3$ corner of the phase noise spectrum (Section D). We discuss the quantification of noise sideband imbalance based on simultaneous AM and FM conditions (Section E).

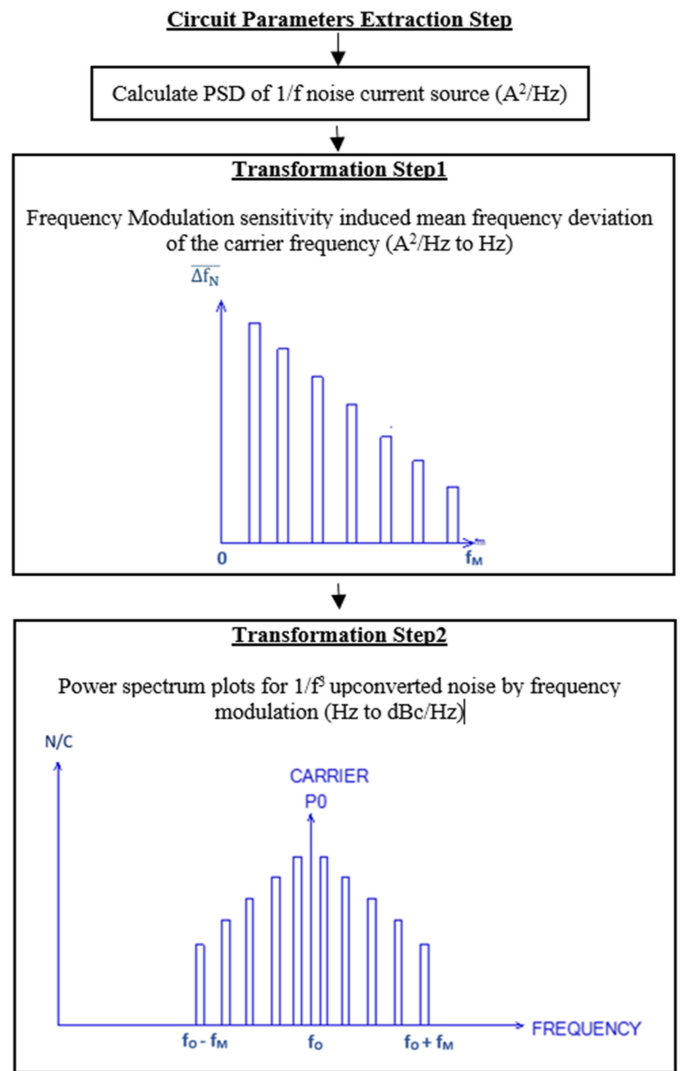


FIGURE 5. LC VCO narrowband FM induced $1/f^3$ phase noise transformational flow.

A. THERMAL PHASE NOISE ANALYSIS BY THE MACROSCOPIC TRANSFORMATIONAL METHOD

The circuit parameters extraction step involves the conversion of the oscillator's macroscopic temperature into a total thermally induced noise PSD from the summation of noise contributions of the passive LC tank and active components within the LC VCO circuit. The total PSD can be expressed in its general form as [1]

$$PSD = \sum S_V(f) = 4kTR_pF_N \quad (1)$$

where $S_V(f)$ is expressed as mean-square noise voltage density in V^2/Hz from the individual noise sources within the oscillator's circuit, k is Boltzmann's constant, T is ambient temperature in degrees Kelvin, R_p is the equivalent parallel resistance of the tank and F_N is the excess noise factor.

1) THE STATIC METHOD FOR DETERMINING PHASE NOISE

This section describes our unique method of determining the phase noise associated with a noisy free-running oscillator. Our method of calculating how the thermal noise PSD in (1) is transformed into phase noise using Adler's equation [26] as a transformational block is called the "static method".

In 1946, R. Adler created a classic differential equation known as Adler's equation to model an oscillator's phase difference resulting from an injected signal. When a free running oscillator is perturbed by an injected signal, the locking dynamics are given by [30]–[32]

$$\frac{1}{2\pi} \frac{d\Delta\varphi(t)}{dt} = \Delta f_{NT} - \frac{f_O}{2Q} \frac{V_{inj}}{V_O} \sin(\Delta\varphi(t)) \quad (2)$$

where $\Delta\varphi(t)$ is the instantaneous phase difference between the injected signal and the oscillator's carrier signal, Δf_{NT} is the frequency deviation of the carrier due to random thermal noise injection, f_O is the oscillator's free running carrier frequency and Q is the quality factor of the resonant LC tank circuit. The instantaneous amplitude of the injected noise signal is V_{inj} and the output amplitude of oscillator carrier voltage is V_O . It follows from (2) that general Adler's equation has a time dependence. We term this equation as the "dynamic Adler equation" because it provides insight into the locking dynamics. It provides an estimation of the locking range of the oscillators for a given injection signal.

TPN theory evaluates the oscillator's response to noise sources generated on the die itself such as thermal noise and $1/f$ noise occurring at the various transistors where the phase of the injected noise is continuously changing and cannot be predicted. In a way similar to Error Vector Magnitude (EVM) systems testing [33], we consider the noise voltages serving as the injection port input. We can think of the noise voltage as being displayed on an I/Q axis. As in the case of EVM measurements the randomly changing noise voltage lies within a circle centered at the origin of the I/Q axis. This continuously changing noisy voltage, representing an ever-changing phase of the injection port signal, lies within a circle centered on the zero point of the I/Q axis and has phase values that over time cancel each other out. This means there is no discernible fixed value of phase associated with the noise injection within the noise circle.

Assuming the injected signal is a noise source (such as thermal noise) means the injection phase continues to always change without stopping or returning to a previous value. It does not have a definite repeatable value and is no longer a well-defined function of time. In fact, over a reasonable period of time, the phase of this injected signal will average to zero. With the injection signal phase now set to zero, and the oscillator's phase remaining a constant, the time derivative of $\Delta\varphi(t)$ with respect to time becomes zero in (2). We term this version of the Adler equation as the "static Adler equation". Under these conditions the oscillator will always operate at its free-running frequency.

2) TRANSFORMATION STEP 1

Step 1 converts the total macroscopic thermal noise PSD into a random frequency deviation using the Static Adler equation.

In TPN analysis, the locking width and the frequency deviation as a result of the phase noise are intimately related. The correspondence of injection locking bandwidth and phase noise induced frequency deviation can be understood based on the fact that the phase of the injected noise we have considered is continuously changing and averages out to zero net phase shift. However, at any point in time the V_{inj} phase may have a value lasting for a very short time period, which we call a "coherence moment". It is during one of these "coherence moments" that V_{inj} 's momentary phase will briefly pull the carrier frequency away from its free-running value. The injected noise can then briefly open a locking window. However, that window is filled with noise. An increase in amplitude of the noise will increase the locking width. It will not change the carrier frequency.

Each time a "coherence moment" occurs, the carrier frequency will momentarily be pulled towards the injected noise signal. This process continues to occur randomly right up to the full extent of the locking range, but no farther. Phase noise is created as the result of this noisy frequency deviation of the carrier frequency, which has a maximum value equal to the full extent of the locking range. However, "coherence moments" will also occur for V_{inj} offsets which are less than the full locking range. It is in these interior "coherence moments" that the injection locking bandwidth gets filled with noise. The result is that the full locking range is completely filled with the phase noise that is being transformed from the IC's thermal and $1/f$ noise. The mean maximum noisy frequency deviation of the LC oscillator (resulting from the noisy signal) is exactly equal to the locking width of the oscillator.

Once the injection locked oscillator has settled into a steady state, $\Delta\varphi(t)$ is constant and (2) can be simplified to the "static Adler equation" as

$$\Delta f_{NT} = \frac{f_O}{2Q} \frac{V_{inj}}{V_O} \sin(\Delta\varphi(t)) \quad (3)$$

The maximum frequency deviation as the full extent of the locking width, Δf_{NTmax} , is found from the orthogonal relation of $\Delta\varphi(t) = 90^\circ$, and is expressed as

$$\Delta f_{NTmax} = \frac{f_O}{2Q} \frac{V_{inj}}{V_O} \quad (4)$$

For the purpose of calculating the thermal phase noise of a free running oscillator we consider the critical 1 Hz band slice at the very edge of the locking range Δf_{NTmax} . Locking the free running oscillator to this critical thermal noise power slice will lead to a maximum phase noise frequency deviation. The random maximum mean frequency deviation, $\overline{\Delta f_{NTmax}}$ due to all thermal noise sources in the LC oscillator can be expressed based on (4) and modifying it to be

$$\overline{\Delta f_{NTmax}^2} = \left(\frac{f_O}{2Q} \right)^2 \frac{\sum V_{inj_1Hz}^2}{V_O^2} \quad (5)$$

where $\overline{\sum V_{inj,1Hz}^2} = \sum S_v(f)$ is the total injected mean-square thermal noise PSD defined in (1). Combing (5) and (1) we get

$$\overline{\Delta f_{NTmax}^2} = \left(\frac{f_O}{2Q}\right)^2 \frac{4kTR_P F_N}{V_O^2} \quad (6)$$

Denoting $\overline{P_N} = 4kTF_N$ as the total macroscopic thermal noise power measured in a one-hertz wide band-pass filter, and $P_O = V_O^2/R_P$ as the oscillator's carrier output power, we arrive at

$$\overline{\Delta f_{NTmax}^2} = \left(\frac{f_O}{2Q}\right)^2 \frac{\overline{P_N}}{P_O} \quad (7)$$

The essential concept is that the ratio of $\overline{P_N}$ to P_O determines the random maximum mean noise frequency deviation $\overline{\Delta f_{NTmax}}$. This induces stochastic phase-shifts and by consequence, phase-modulation of the output signal resulting in phase noise.

3) TRANSFORMATION STEP 2

Step 2 is to convert the $\overline{\Delta f_{NTmax}^2}$ into the single-sideband noise-to-carrier-power-ratio $(N/C)_T$. This transformation is done within the bounds of small-signal FM theory. In the case of small-signal FM modulation, there are only two FM noise sidebands generated symmetrically about the carrier [27]. The ratio between the power in each of these noise side-tone and the carrier power is given by

$$(N/C)_T = \frac{1}{4} \frac{\overline{\Delta f_{NTmax}^2}}{f_M^2} \quad (8)$$

where f_M is the modulation deviation rate, which is the same as the noise sideband's offset frequency from the carrier. By combining (6) and (8), we arrive at the final expression for the thermal phase noise $(N/C)_T$ as (9). It is evident from (9) that our transformational method of thermally induced phase noise derivation results in the same equation as Leeson [12] originally postulated with the scaler conversion of the noise factor $F = F_N/4$. The thermal phase noise is reduced as both the carrier amplitude V_O and Q increase as predicted in (9)

$$\left(\frac{N}{C}\right)_T = \frac{1}{4} \frac{4kTR_P F_N}{V_O^2} \left(\frac{f_O}{2Qf_M}\right)^2 = \frac{4kTR_P F}{V_O^2} \left(\frac{f_O}{2Qf_M}\right)^2 \quad (9)$$

where the phase noise power spectrum $10\log_{10}((N/C)_T)$ in dBc/Hz exhibits a slope of 20 dB per decade with offset frequency, f_M . The phase noise is scaled by the specific noise factor F in (9), which has been extracted for an LC oscillator [13] from the noise model of a mixer with a switching differential pair. This noise factor F is given in [13]

$$F = 2 + \frac{8}{9} \gamma g_{m_bias} R_P + \frac{8I_{bias} R_P \gamma}{\pi V_O} \quad (10)$$

Here γ is the coefficient of channel thermal noise, g_{m_bias} is the transconductance of the tail bias current-source transistor M_5 , and I_{bias} is the tail bias current. The steps of the proposed

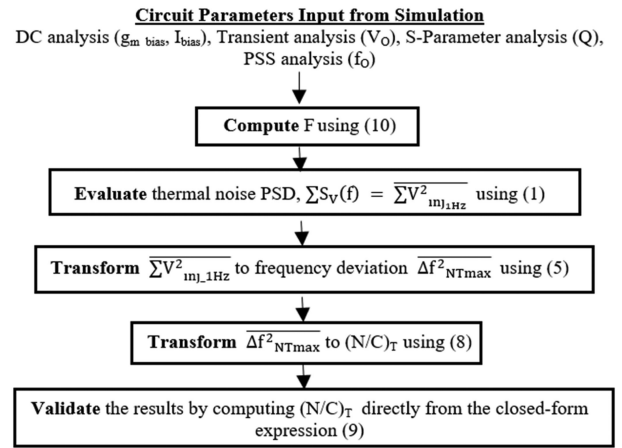


FIGURE 6. Computational flow for thermal phase noise.

computational algorithm for thermal phase noise are shown in Fig. 6.

One of the limitations of our TPN theory is that the power spectrum in (9) risks going to ∞ at zero offset frequency f_M and is not able to predict the Lorentzian shape of the oscillator output voltage. This is because the small-signal approximation is no longer valid as f_M approaches zero. Introducing non-linear effects associated with violating the small-signal approximation is expected to prevent a value of ∞ from occurring at zero offset frequency. The readers are encouraged to refer to [21] to understand the Lorentzian spectrum of oscillator thermal phase noise.

B. AM UP CONVERTED PHASE NOISE ANALYSIS BY THE MICROSCOPIC TRANSFORMATIONAL METHOD

In this section we quantify the close-in $1/f^3$ phase noise into a closed-form expression for a LC VCO operating in its latent role as an amplitude modulator. In our analysis we have chosen the tail-bias transistor M_5 as the microscopic flicker noise source. The circuit parameters extraction step is to calculate the PSD of the baseband $1/f$ noise current source $\overline{I_{n1/f}^2}$ from (11) in A^2/Hz [1] using circuit parameters.

$$\overline{I_{n1/f}^2} = g_{m_bias}^2 \left(\frac{K_f}{C_{ox} W L f_M} \right) \quad (11)$$

where K_f is a process-dependent constant, C_{ox} is the gate oxide capacitance per unit area, W and L are the width and length of the MOS device respectively. The flicker noise is obtained by simulation where it is modeled as a voltage source $\overline{V_{n1/f}^2}$ in V^2/Hz [1] in series with the gate of M_5 and is related to drain noise current PSD in (11) as

$$\overline{I_{n1/f}^2} = g_{m_bias}^2 * \overline{V_{n1/f}^2} \quad (12)$$

1) TRANSFORMATION STEP 1

Step 1 is to evaluate the up-converted noise sidebands about the carrier frequency. The modulation transformation process is first measured (by simulation) for an infinitesimal test

current being injected at the drain of the circuit transistor which has been chosen for $(1/f)$ noise injection. The injected test current mimics the change in the bias current which is caused by the $1/f$ noise injection. Injecting this small dc test current at this point in the circuit (small enough to maintain linearity) will enable the calculation of the rate of change of the oscillator's carrier current amplitude signal with respect to a change in the bias current. The modulation sensitivity of the infinitesimal change in amplitude of the oscillator's carrier output current with respect to the infinitesimal dc test current flowing in the transistor of choice causing the change is obtained by simulation and is represented as

$$\frac{\partial I_O}{\partial i} \quad (13)$$

The PSD of the up-converted injected noise current sidebands around the carrier frequency is the result of the modulation by the baseband $(1/f)$ noise current injection at very low frequencies (close to DC) and can be obtained from (11) and (13) as

$$\overline{I_{inj_up}^2} = \overline{I_{n1/f}^2} \left(\frac{\partial I_O}{\partial i} \right)^2 \quad (14)$$

where $\overline{I_{inj_up}^2}$ represents the up-converted flicker noise sidebands PSD in A^2/Hz .

2) TRANSFORMATION STEP 2

The second transformational step is to convert the microscopic up-converted flicker noise sidebands PSD $\overline{I_{inj_up}^2}$ into a random frequency deviation of the carrier based on Adler's static injection locking theory in its current form [26]. For the purpose of calculating the $1/f^3$ phase noise in a free running oscillator which has been injection locked to its own up-converted $(1/f)$ noise source, we need to consider the 1 Hz band at the very edge of the locking range. This leads to a random maximum mean frequency deviation Δf_{NF_max}

$$\Delta f_{NF_max} = \frac{f_O}{2Q} \frac{I_{inj}}{I_O} \quad (15)$$

where I_{inj} is the injected noise current signal strength and I_O is the carrier's output current.

The maximum mean frequency deviation of the carrier, $\Delta f_{NF_AM_max}$, due to the microscopic up-converted $(1/f)$ noise current injection with amplitude modulation is obtained by modifying (15) as

$$\overline{\Delta f_{NF_AM_max}^2} = \left(\frac{f_O}{2Q} \right)^2 \frac{\overline{I_{inj_up}^2}}{I_O^2} \quad (16)$$

Replacing $\overline{I_{inj_up}^2}$ from (14) in (16) we have

$$\overline{\Delta f_{NF_AM_max}^2} = \left(\frac{f_O}{2Q} \right)^2 \overline{I_{n1/f}^2} \left(\frac{\partial I_O}{\partial i} \right)^2 \left(\frac{1}{I_O} \right)^2 \quad (17)$$

The concept here is that the ratio of microscopic up-converted flicker noise average power $\overline{I_{inj_up}^2}$ measured by

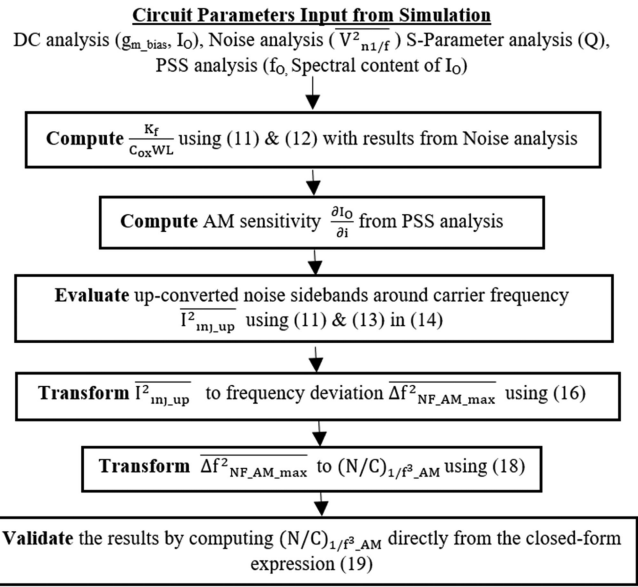


FIGURE 7. Computational flow for AM upconverted $1/f^3$ phase noise.

using a one-hertz wide band-pass filter, to the oscillator's carrier output power I_O^2 , determines the maximum mean noise frequency deviation $\Delta f_{NF_AM_max}$. The mean maximum frequency deviation of the LC oscillator (resulting from the noisy baseband signal) is exactly equal to the locking width of the oscillator under this situation.

3) TRANSFORMATION STEP 3

The final transformational step is to convert the $\overline{\Delta f_{NF_AM_max}^2}$ into single-sideband noise-to-carrier-power-ratio $(N/C)_{1/f^3_AM}$. The ratio between the power of each noise sideband and the power of the carrier based on small-signal FM modulation theory [27] is given by

$$(N/C)_{1/f^3_AM} = \frac{1}{4} \frac{\overline{\Delta f_{NF_AM_max}^2}}{f_M^2} \quad (18)$$

After combining (11), (17) and (18) we obtain the final expression for transformational AM up-converted $1/f^3$ phase noise

$$\begin{aligned} (N/C)_{1/f^3_AM} &= \frac{1}{4} \left(\frac{f_O}{2Q} \right)^2 g_{m_bias}^2 \left(\frac{K_f}{C_{ox}WL} \right) \left(\frac{\partial I_O}{\partial i} \right)^2 \left(\frac{1}{I_O} \right)^2 \left(\frac{1}{f_M} \right)^3 \end{aligned} \quad (19)$$

where the phase noise power spectrum $10 \log_{10}((N/C)_{1/f^3_AM})$ in dBc/Hz exhibits a slope of 30 dB per decade with offset frequency f_M . The steps of the computational algorithm for AM upconverted $1/f^3$ phase noise are shown in Fig. 7.

C. FM UP CONVERTED PHASE NOISE ANALYSIS

In this section we quantify the close-in $1/f^3$ phase noise closed-form expression for the LC VCO operating in its latent role as a narrow-band frequency modulator.

1) TRANSFORMATION STEP 1

The first transformation is to derive the frequency deviation of the VCO by calculating the oscillator's frequency sensitivity to an infinitesimal test current injection at the drain of M_5 by simulation. The Q factor of the resonator is buried within this frequency sensitivity. The FM process itself directly produces a frequency deviation, and hence the Adler's static injection equation is not needed in this case. The injected dc test current is analogous to the change in the dc bias current caused by the (1/f) noise. The free running oscillators' carrier frequency sensitivity to the test current change in the selected transistor, due to frequency modulation, is

$$\frac{\partial f_O}{\partial i} \quad (20)$$

The random mean frequency deviation of the carrier, $\overline{\Delta f_{NF_FM}}$, produced by the (1/f) noise acting in the transistor of choice is

$$\overline{\Delta f_{NF_FM}^2} = \overline{I_{n1/f}^2} \left(\frac{\partial f_O}{\partial i} \right)^2 \quad (21)$$

2) TRANSFORMATION STEP 2

The final transformation step is to convert the $\overline{\Delta f_{NF_FM}^2}$ into single-sideband noise-to-carrier-power-ratio $(N/C)_{1/f^3_FM}$. The ratio between the power of each noise sideband and the power in the carrier based on small-signal FM modulation theory [27] is given by

$$(N/C)_{1/f^3_FM} = \frac{1}{4} \frac{\overline{\Delta f_{NF_FM}^2}}{f_M^2} \quad (22)$$

After combining (11), (21) and (22), the final expression for transformational FM up-converted $1/f^3$ phase noise is

$$(N/C)_{1/f^3_FM} = \frac{1}{4} g_{m_bias}^2 \left(\frac{K_f}{C_{ox}WL} \right) \left(\frac{\partial f_O}{\partial i} \right)^2 \left(\frac{1}{f_M} \right)^3 \quad (23)$$

The phase noise power spectrum $10\log_{10}((N/C)_{1/f^3_FM})$ in dBc/Hz exhibits a slope of 30 dB per decade with an offset frequency of f_M from the carrier. The steps of the proposed computational algorithm for FM upconverted $1/f^3$ phase noise are shown in Fig. 8.

D. $1/f^3$ CORNER OF PHASE NOISE SPECTRUM

In the case when (1/f) AM upconverted phase noise is dominant over (1/f) FM upconverted phase noise, the $1/f^3$ phase noise corner frequency (f_{CAM}) can be determined from equating (9) and (19) and solving for $f_M = f_{CAM}$, resulting in

$$f_{CAM} = g_{m_bias}^2 \left(\frac{K_f}{C_{ox}WL} \right) \left(\frac{\partial I_O}{\partial i} \right)^2 \left(\frac{1}{I_O} \right)^2 \frac{V_O^2}{4kTR_pF_N} \quad (24)$$

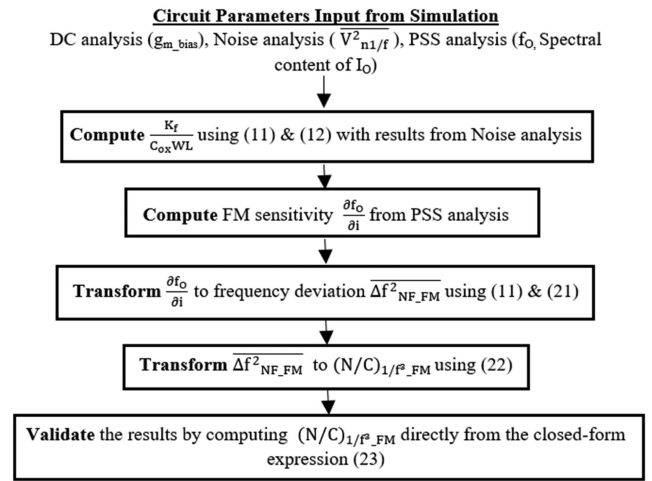


FIGURE 8. Computational flow for FM upconverted $1/f^3$ phase noise.

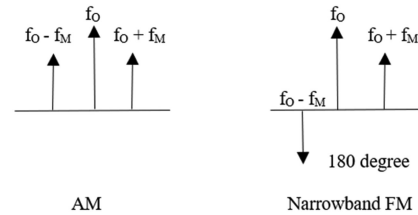


FIGURE 9. Spectra of AM and narrowband FM signals.

In the second case where FM noise sideband modulation is dominant over AM, the $1/f^3$ phase noise corner frequency (f_{CFM}) after equating (9) and (23) and solving for $f_M = f_{CFM}$ is

$$f_{CFM} = g_{m_bias}^2 \left(\frac{K_f}{C_{ox}WL} \right) \left(\frac{\partial f_O}{\partial i} \right)^2 \left(\frac{2Q}{f_0} \right)^2 \frac{V_O^2}{4kTR_pF_N} \quad (25)$$

E. SIMULTANEOUS AM AND FM NOISE MODULATION AND NOISE SIDEBAND IMBALANCE

Pure AM or FM signals always have equal sidebands, but when the two are present together, the modulation vectors usually add up in one sideband and subtract in the other [27]. Thus, unequal noise sidebands indicate the simultaneous presence of both types of upconverted $1/f$ noise, AM and FM. Only in the unusual case when FM and AM phase noise have about the same value must their relationship be taken into account. Fig. 9 shows the spectra of AM and FM signals. Both the upper and the lower AM sidebands are at 0° of phase relative to each other. However, in the FM case, the upper sideband is at 0° relative to the AM upper sideband, but the FM lower sideband is at 180° relative to the lower AM noise sideband. This means if the AM phase noise and the FM phase noise happen to be of about the same magnitude, the combined upper noise sideband would be doubled (i.e., 3dB increase), but the two lower sidebands would cancel each

TABLE 1. Parameters of the LC Oscillator

ELEMENTS	VALUES
W/L (M1, M2)	12u/0.18u
W/L (M3, M4)	24u/0.18u
W/L (M5)	192u/0.18u
L	1.25nH
r_S	6Ω
$C_{VAR} @ V_{TUNE} = 650mV$	63fF
C_0, C_1, C_2, C_3	135fF, 215fF, 305fF, 456fF

other out, resulting in a single sideband phase noise spectrum with only the upper sideband being present.

The TPN theory has the ability to indicate the degree of balance based on a calculation of $(N/C)_{1/f^3_AM}$ from (19) and $(N/C)_{1/f^3_FM}$ from (23) and will enable the designers to judge the relative ratio of AM and FM phase noise sideband modulation.

V. NUMERICAL EXAMPLE

In this section the accuracy of the proposed transformational phase noise analysis is investigated in connection with the benchmark CMOS cross-coupled LC VCO topology shown in Fig. 2. The differential outputs OUT+ and OUT- are driving a 100Ω load. The parameters of the circuit shown in Fig. 2 are reported in Table 1.

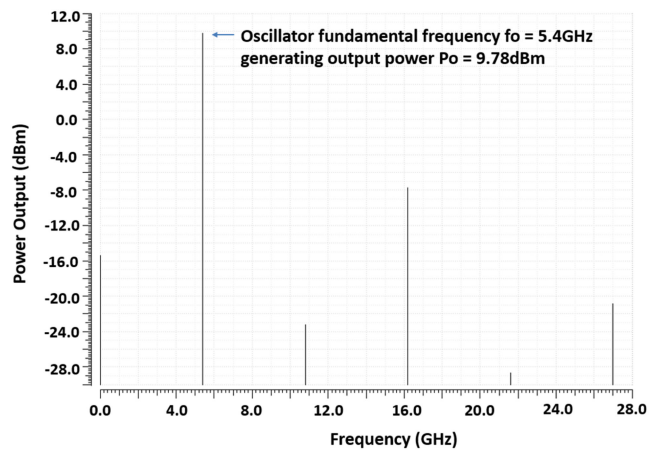
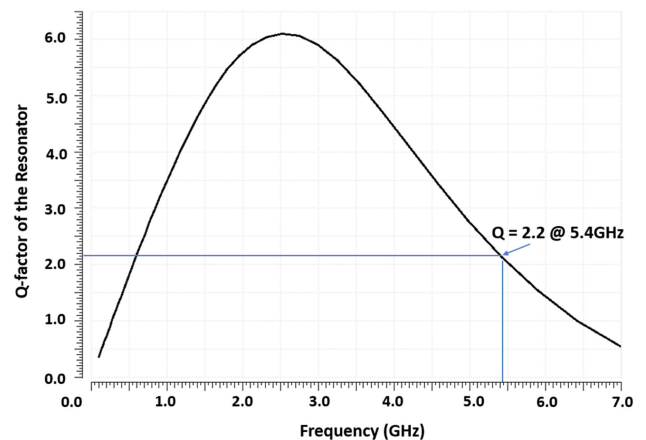
Initially we simulate to obtain the dc parameters for the free-running oscillator operating at a temperature $T = 300^\circ K$ which are required to calculate both thermal and $1/f^3$ phase noise. To this aim, we simulate the dc operating condition of the oscillator with a supply voltage of $V_{DD} = 1.8V$, the dc bias voltage V_{bias} of the tail transistor M_5 set at 712 mV and all the switch capacitors C_0 to C_3 turned on using control bits b_3 – b_0 set to 1111. The simulations were done with a commercially available simulator SpectreRF using an existing 90 nm RFCMOS process technology. The resulting transconductance and bias current of M_5 are $g_{m_bias} = 11.53$ mS and $I_{bias} = 6$ mA respectively. The quiescent carrier current I_0 under these operating conditions is 3 mA.

A. THERMAL PHASE NOISE NUMERICAL ANALYSIS AT THE OFFSET FREQUENCY $f_M = 10$ MHz

1) CIRCUIT PARAMETERS NEEDED TO CALCULATE THERMAL PHASE NOISE

At the first step of our analysis, we simulate the steady-state response of the oscillator using the periodic-steady-state analysis (PSS) of SpectreRF and harmonic balance method [34]. The resulting oscillation frequency is $f_0 = 5.4$ GHz with an output power of $P_0 = 9.78$ dBm, as in Fig. 10.

To verify the accuracy of the transformation thermal phase noise theory we first calculate excess noise factor F as in (10). To this aim, we evaluate the Q-factor of the resonator tank $Q = 2.2$ at $f_0 = 5.4$ GHz using s-parameter simulation as shown in Fig. 11. The transient simulation yields steady-state differential output oscillator swing of $V_O = 1.23$ V as shown

**FIGURE 10. Differential output spectral content of the LC oscillator.****FIGURE 11. Q-factor of the LC-tank resonator.**

in Fig. 12. We derive the equivalent parallel load resistance at the frequency of oscillation to be $R_p \approx (1 + Q^2)r_S = 35$ ohm. Also, γ is approximately 2.5 in our 90 nm process. With these values, we calculate $F = 4$.

2) EFFECT OF VARACTOR AND SWITCH NOISES

In order to include the noise contributions from the varactor and switches we obtained, from s-parameter simulations, the series resistance of the varactor and that of the switches as $r_v = 4.4\Omega$ and $r_{sw} = 6.5\Omega$ respectively. We update the noise factor F after taking into account this additional thermally induced phase noise. The F value gets changed to 4.3

3) THERMALLY INDUCED PHASE NOISE BASED ON TPN THEORY

We use the transformational flow shown in Fig. 3, along with the step-by-step computational procedure shown in Fig. 6 to arrive at $(N/C)_T$ using the circuit parameters obtained in section A.1. The computed variables from TPN theory are listed in Table 2. Using these values, at an offset frequency

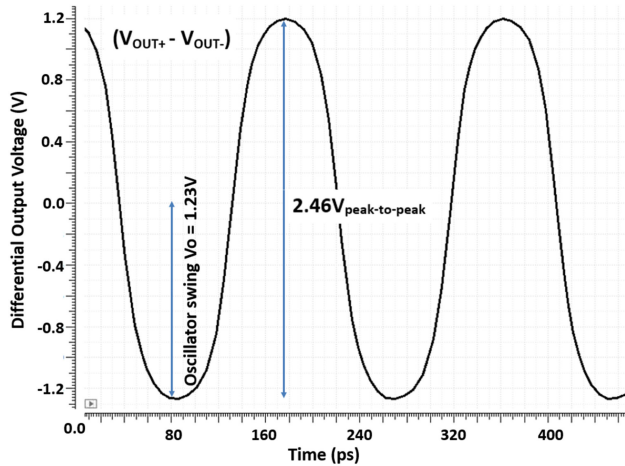


FIGURE 12. Steady-state response of the LC oscillator.

TABLE 2. Computation of Thermal Phase Noise

Computed Variable from TPN theory	Equation Number	Value
$F = F_N/4$	10	4.3
$\overline{\Sigma V_{inj_1Hz}^2} = \Sigma S_V(f)$	1	$9.97E-18 \text{ V}^2/\text{Hz}$
$\overline{\Delta f_{NTmax}}$	6	3.15 Hz
$10\log_{10}((N/C)_T)$	8	-136 dBc/Hz

of $f_M = 10 \text{ MHz}$, we obtain the $1/f^2$ thermal phase noise $10\log_{10}((N/C)_T)$ to be -136 dBc/Hz .

B. AM UP CONVERTED PHASE NOISE NUMERICAL ANALYSIS AT THE OFFSET FREQUENCY $F_M = 1 \text{ KHz}$

1) COMPUTATION OF PSD OF THE TAIL-BIAS $1/f$ NOISE CURRENT

In the first step of our analysis, we determine the flicker noise voltage referred to the gate of M_5 in units of V^2/Hz by means of simulation. The noise simulation of the stand-alone bias transistor M_5 results in $\overline{V_{n1/f}^2} = 2.12E-12 \text{ V}^2/\text{Hz}$ at $f_M = 1 \text{ kHz}$. With this value, we derive the flicker noise current at the drain of M_5 , $\overline{I_{n1/f}^2}$ from (12) as $2.82E-16 \text{ A}^2/\text{Hz}$.

2) COMPUTATION OF THE OSCILLATOR'S AMPLITUDE MODULATION SENSITIVITY

The simulation to evaluate the oscillator amplitude and frequency modulation sensitivities resulting from the upconversion of the $1/f$ noise present in the bias current, is initiated by modulating the gate bias voltage of M_5 . The bias voltage is modulated through a current-controlled voltage source applied at the gate of M_5 . This initiates an infinitesimal small signal test current injection ∂i by means of varying the bias current I_{bias} of M_5 . This is analogous to the change in the bias current in M_5 which is caused by $1/f$ noise. This current injection will result in a change in the amplitude of the oscillator's

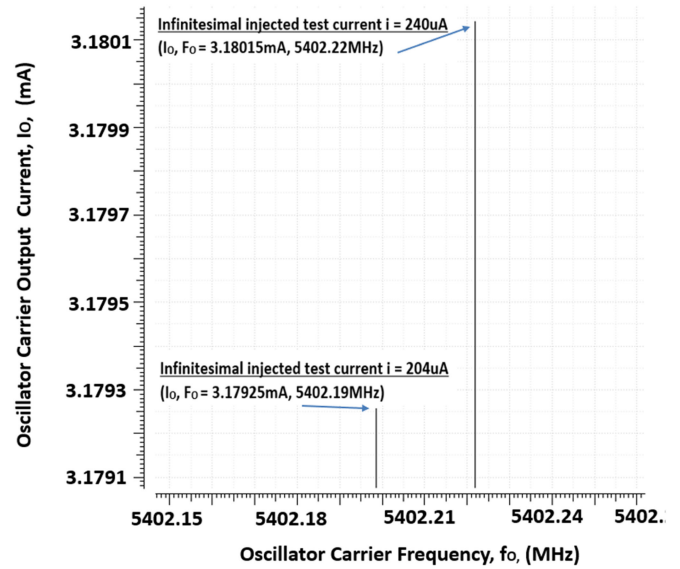


FIGURE 13. Spectra of the LC oscillator carrier current with varying infinitesimal test current injection at the bias transistor M_5 .

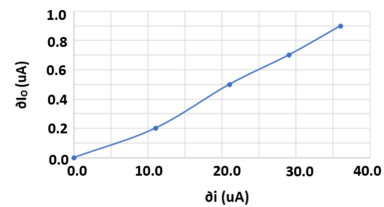


FIGURE 14. Oscillator AM sensitivity plot.

carrier output current I_O and the frequency of the carrier f_O . The simulation results in Fig. 13 show the variation of the carrier current amplitude I_O and the carrier frequency f_O due to the injection of a dc test current at the drain of M_5 . These results will be used to calculate the AM and FM modulation sensitivities. The oscillator's carrier current sensitivity is plotted in Fig. 14, the slope of which determines the oscillator's amplitude modulation sensitivity to be $\partial I_O/\partial i = 0.025$.

3) AM INDUCED PHASE NOISE BASED ON TPN THEORY

We use the transformational flow for AM induced phase noise that is shown in Fig. 4, along with the step-by-step computational procedure shown in Fig. 7, to arrive at $(N/C)_{1/f^3_AM}$ using the circuit parameters obtained in section B.1 and B.2. The computed variables from TPN theory are listed in Table 3. Using these values, we obtain close-in phase noise $10\log_{10}((N/C)_{1/f^3_AM})$ to be -21.3 dBc/Hz at an offset frequency $f_M = 1 \text{ kHz}$.

TABLE 3. Computation of AM Upconverted $1/f^3$ Phase Noise

Computed Variable from TPN theory	Equation Number	Value
$\overline{I_{n1/f}^2}$	12	2.82E-16 A ² /Hz
$\frac{\partial I_O}{\partial i}$	13	0.025
$\overline{(I_{in_up})^2}$	14	1.76E-19 A ² /Hz
$\overline{\Delta f_{NF_AM_max}}$	17	172 Hz
$10\log_{10}((N/C)_{1/f^3_AM})$	18	-21.3 dBc/Hz

TABLE 4. Computation of FM Upconverted $1/f^3$ Phase Noise

Computed Variable from TPN theory	Equation Number	Value
$\frac{\partial f_O}{\partial i}$	20	0.83GHz/Amp
$\overline{\Delta f_{NF_FM}}$	21	14 Hz
$10\log_{10}((N/C)_{1/f^3_FM})$	22	-43 dBc/Hz

TABLE 5. Comparison of Computation Results Using TPN Theory Versus Simulation Results From SpectreRF

Parameters	Computation from TPN theory	Simulation from SpectreRF
Phase noise at offset frequency = 1kHz	-21.3 dBc/Hz	-23.4 dBc/Hz
Phase noise at offset frequency = 10MHz	-136 dBc/Hz	-135.9 dBc/Hz
$1/f^3$ corner frequency	2.6 MHz	2.1 MHz

C. FM UP CONVERTED PHASE NOISE NUMERICAL ANALYSIS AT THE OFFSET FREQUENCY $f_M = 1$ KHz

1) COMPUTATION OF THE OSCILLATOR'S FREQUENCY MODULATION SENSITIVITY

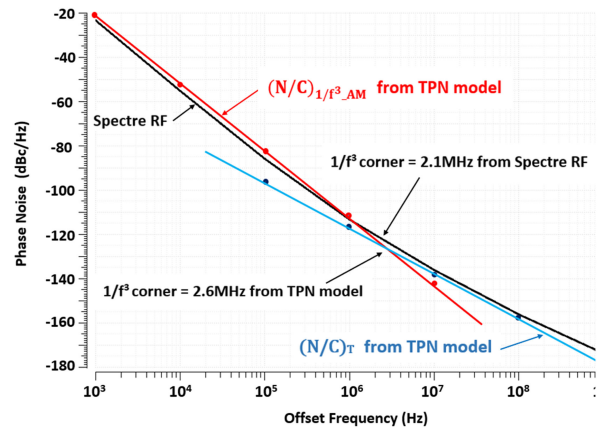
We compute the oscillator frequency modulation sensitivity to be $\partial f_O/\partial i = 0.83$ GHz/Amp from Fig. 13.

2) FM INDUCED PHASE NOISE BASED ON TPN THEORY

We use the transformational flow for FM induced phase noise that is shown in Fig. 5, along with the step-by-step computational procedure shown in Fig. 8 to arrive at the $(N/C)_{1/f^3_FM}$ using the circuit parameters obtained in section C.1. The computed variables from TPN theory are listed in Table 4. Using these values, we obtain $10\log_{10}((N/C)_{1/f^3_FM})$ to be -43 dBc/Hz. at an offset frequency of $f_M = 1$ kHz.

D. $1/f^3$ CORNER OF PHASE NOISE SPECTRUM

In this example we have considered the FM upconverted $1/f$ noise is considerably below the AM upconverted $1/f$ noise and so it can be safely ignored. The $1/f^3$ corner frequency is thus obtained from (24) as $f_{CAM} = 2.6$ MHz.


FIGURE 15. Phase noise spectrum of the LC VCO: simulated with the Noise of SpectreRF, computed with the TPN theory model.

E. PHASE NOISE SPECTRUM OF THE FREE RUNNING LC OSCILLATOR

The predicted phase noise performance of the CMOS LC VCO topology in Fig. 2 with the parameters of the circuit as reported in Table 1 was verified using the PSS and Pnoise analysis of SpectreRF. Fig. 15 shows the phase noise values calculated using the analytical formulas (9) and (19), and compares them to the phase noise values derived with SpectreRF. From Fig. 15 we see that analytically computed curves closely match, with good accuracy, with the simulation results and confirm the correctness of the proposed TPN theory. In particular, we see that the proposed calculation yields a phase noise spectrum falling with a slope of 30 dB/decade at low frequency offsets and with a slope of 20 dB/decade at high frequency offsets as expected. The $1/f^3$ corner frequency is calculated from (24). A summary of the analytical computations and simulation values are listed in Table 5.

VI. CONCLUSION

In this paper, we present a unique theoretical approach for calculating the output phase noise of LC oscillators. The theory evaluates the oscillator's response to two noise sources generated on the die itself, thermal noise and $1/f$ noise occurring at the various transistors where the phase of the injected noise is continuously changing randomly.

The basic philosophy of our procedure is that oscillators produce phase noise as a direct result of their non-ideal latent natures working together with certain internal self-supplied noise sources associated with various circuit components. The proposed TPN theory together with its final closed-form phase noise expressions allow circuit designers to easily identify the noise sources and estimate their contributions to the oscillator's overall phase noise. It also provides the flexibility for designers to selectively apply the TPN theory to independently calculate either thermal or $1/f^3$ phase noise or both, as required for their applications.

Our transformational theory is demonstrated and validated by using a practical 90 nm process CMOS LC VCO example

which can be extended to other process technologies and other circuit topologies for example in LC Colpitts oscillators. Also, we have chosen the tail-bias transistor M5 in Fig. 2 to be the dominant contributor of $1/f^3$ phase noise spectrum in the LC VCO. But as we move to process nodes of less than 45 nm, depending on oscillator implementation, either the MOS switching differential pair or the tail bias transistor's flicker noise contributions may dominate the near-carrier phase noise. In this scenario, we will have to modify the oscillator's amplitude and frequency modulation sensitivities.

The accuracy of the proposed method is verified by comparing it with the periodic noise analysis of the SpectreRF simulator. While several methods for the phase noise computation already exist, they either involve highly detailed numerical analysis or are based on mathematically challenging models which are unavailable to most circuit designers. Our TPN theory enables a designer to accurately calculate the phase noise of a free running LC oscillators by using simple analog simulation capabilities together with closed form equations to gain design insights by quickly repeating calculations under a number of variant conditions. This methodology provides the designers clear insight and understanding of how phase noise mechanisms become modified at each step in the transformation process. This capability will guide the designers of various low phase noise oscillators by providing greater flexibility in evaluating optimal circuit element placements and their values.

REFERENCES

- [1] B. Razavi, *RF Microelectronics*, 1st ed. Hoboken, NJ, USA: Prentice-Hall, 1998. ch. 7.
- [2] T. H. Lee, *The Design of CMOS Radio-Frequency Integrated Circuits*, 2nd ed. Cambridge, U.K.: Cambridge Univ. Press, 2003.
- [3] Y. Huo, X. Dong, L. Li, M. Xie, and W. Xu, "26/40 GHz CMOS VCOs design of radio front-end for 5G mobile devices," in *Proc. IEEE Int. Conf. Ubiquitous Wireless Broadband (ICUWB)*, 2016, pp. 1–4.
- [4] Z. Chen, H. Chen, B. Li, Y. Li, Z. Wu, and Y. Xu, "Design of a 24–30 GHz wide tuning-range VCO for 5G millimeter wave communication," in *Proc. IEEE Int. Conf. Microw. Millimeter Wave Technol. (ICMMT)*, 2019, pp. 1–3.
- [5] K. A. Kouznetsov and R. G. Meyer, "Phase noise in LC oscillators," *IEEE J. Solid-State Circuits*, vol. 35, no. 8, pp. 1244–1248, Aug. 2000.
- [6] C. Samori, A. L. Lacaita, F. Villa, and F. Zappa, "Spectrum folding and phase noise in LC tuned oscillators," *IEEE Trans. Circuits Syst. II, Analog Digit. Signal Process.*, vol. 45, no. 7, pp. 781–790, Jul. 1998.
- [7] Q. Huang, "Phase noise to carrier ratio in LC oscillators," *IEEE Trans. Circuits Syst. I, Fundam. Theory Appl.*, vol. 47, no. 7, pp. 965–980, Jul. 2000.
- [8] P. Andreani, X. Wang, L. Vandl, and A. Fard, "A study of phase noise in colpitts and LC-tank CMOS oscillators," *IEEE J. Solid-State Circuits*, vol. 40, no. 5, pp. 1107–1118, May 2005.
- [9] P. Andreani and A. Fard, "More on the $1/f^2$ phase noise performance of CMOS differential-pair LC-tank oscillators," *IEEE J. Solid-State Circuits*, vol. 41, no. 12, pp. 2703–2712, Dec. 2006.
- [10] S. Saha, S. Krishnan, and A. A. Sweet, "A C-band wide locking range injection locked oscillator-based phase shifter," in *Proc. IEEE Int. Conf. Microw., Antennas, Commun. Electron. Syst. (COMCAS)*, Tel-Aviv, Israel, Nov. 2017, pp. 1–5.
- [11] S. Saha, S. Krishnan, and A. A. Sweet, "A triple mode wide locking range, low phase noise injection locked oscillator-based phase shifter covering the sub-6 GHz 5G bands," in *Proc. IEEE 11th Latin Amer. Symp. Circuits Syst. (LASCAS)*, San Jose, CA, USA, Feb. 2020, pp. 1–4.
- [12] D. B. Leeson, "A simple model of feedback oscillator noise spectrum," *Proc. IEEE*, vol. 54, no. 2, pp. 329–330, Feb. 1966.
- [13] J. J. Rael and A. A. Abidi, "Physical processes of phase noise in differential LC oscillators," in *Proc. IEEE Custom Integr. Circuits Conf.*, May 2000, pp. 569–572.
- [14] D. Murphy, J. J. Rael, and A. A. Abidi, "Phase noise in LC oscillators: A phasor-based analysis of a general result and of loaded Q," *IEEE Trans. Circuits Syst. I, Reg. Papers*, vol. 57, no. 6, pp. 1187–1203, Jun. 2010.
- [15] A. Hajimiri and T. H. Lee, "A general theory of phase noise in electrical oscillators," *IEEE J. Solid-State Circuits*, vol. 33, no. 2, pp. 179–194, Feb. 1998.
- [16] A. Hajimiri and T. H. Lee, "Oscillator phase-noise: A tutorial," *IEEE J. Solid-State Circuits*, vol. 35, no. 3, pp. 326–336, Mar. 2000.
- [17] P. Maffezzoni, "Analysis of oscillator injection locking through phase-domain impulse-response," *IEEE Trans. Circuits Syst. I, Reg. Papers*, vol. 55, no. 5, pp. 1297–1305, Jun. 2008.
- [18] P. Maffezzoni and D. D'Amore, "Evaluating pulling effects in oscillators due to small-signal injection," *IEEE Trans. Comput.-Aided Design Integr. Circuits Syst.*, vol. 28, no. 1, pp. 22–31, Jan. 2009.
- [19] P. Maffezzoni, S. D'Amore, and M. P. Kennedy, "Analysis and design of injection locked frequency dividers (ILFDs) by means of a phase-domain macromodel," *IEEE Trans. Circuits Syst. I Reg. Papers*, vol. 57, no. 11, pp. 2956–2966, Nov. 2010.
- [20] A. Mirzaei, M. E. Heidari, and A. A. Abidi, "Analysis of oscillators locked by large injection signals: Generalized Adler's equation and geometrical interpretation," in *Proc. IEEE Custom Integr. Circuits Conf.*, 2006, pp. 737–740.
- [21] A. Mirzaei and A. A. Abidi, "The spectrum of a noisy free-running oscillator explained by random frequency pulling," *IEEE Trans. Circuits Syst. I, Reg. Papers*, vol. 57, no. 3, pp. 642–653, Mar. 2010.
- [22] A. Demir, A. Mehrotra, and J. Roychowdhury, "Phase noise in oscillators: A unifying theory and numerical methods for characterization," *IEEE Trans. Circuits Syst. I, Fundam. Theory Appl.*, vol. 47, no. 5, pp. 655–674, May 2000.
- [23] A. Demir and J. Roychowdhury, "A reliable and efficient procedure for oscillator PPV computation, with phase noise macromodeling applications," *IEEE Trans. Comput.-Aided Design Integr. Circuits Syst.*, vol. 22, no. 2, pp. 188–197, Feb. 2003.
- [24] O. Suvak and A. Demir, "On phase models for oscillators," *IEEE Trans. Comput.-Aided Design Integr. Circuits Syst.*, vol. 30, no. 7, pp. 972–985, Jul. 2011.
- [25] P. Vanassche, G. Gielen, and W. Sansen, "On the difference between two widely publicized methods for analyzing oscillator phase behavior," in *Proc. IEEE/ACM Int. Conf. Comput.-Aided Design (ICCAD)*, San Jose, CA, USA, Nov. 2002, pp. 229–233.
- [26] R. Adler, "A study of locking phenomena in oscillators," *Proc. IRE*, vol. 34, no. 6, pp. 351–357, 1946.
- [27] *Spectrum Analysis Amplitude and Frequency Modulation*, Application Note, Keysight Technologies Inc., Santa Rosa, CA, USA.
- [28] A. Bevilacqua and P. Andreani, "An analysis of $1/f$ noise to phase noise conversion in CMOS harmonic oscillators," *IEEE Trans. Circuits Syst. I, Reg. Papers*, vol. 59, no. 5, pp. 938–945, May 2012.
- [29] N. N. Tchamov and N. T. Tchamov, "Technique for flicker noise up-conversion suppression in differential LC oscillators," *IEEE Trans. Circuits Syst. II, Exp. Brief.*, vol. 54, no. 11, pp. 959–963, Nov. 2007.
- [30] P. Bhansali and J. Roychowdhury, "Gen-Adler: The generalized Adler's equation for injection locking analysis in oscillators," in *Proc. 14th Asia South Pacific Design Autom. Conf., ASP-DAC*, Yokohama, Japan, Jan. 2009, pp. 522–527.
- [31] D. Dunwell and A. C. Carusone, "Modeling oscillator injection locking using the phase domain response," *IEEE Trans. Circuits Syst. I, Reg. Papers*, vol. 60, no. 11, pp. 2823–2833, Nov. 2013.
- [32] B. Razavi, "A study of injection locking and pulling in oscillators," *IEEE J. Solid-State Circuits*, vol. 39, no. 9, pp. 1415–1424, Sep. 2004.
- [33] M. D. McKinley, "EVM calculation for broadband modulated signals," in *64th ARFTG Conf. Dig.*, Orlando, FL, USA, Dec. 2004, pp. 45–52.
- [34] *Virtuoso Spectre Circuit Simulator RF Analysis User Guide*, Product Version 7.2, Cadence Design Syst., San Jose, CA, USA May 2010.



SUDIPTA SAHA received the B.Tech. degree from the Indian Institute of Technology Kharagpur, Kharagpur, India, in 1991 and the M.E. degree in microelectronics from the Birla Institute of Technology and Science, Pilani, India, in 1995. He is currently working toward the Ph.D. degree in electrical engineering with Santa Clara University, Santa Clara, CA, USA. He has had a successful career record with Panasonic, Huawei, NXP, Lockheed Martin, Foveon and is currently working as a Principal Engineer with Qorvo, San Jose, CA,

USA. He has authored two refereed IEEE conference publications and has reviewed papers for ISCAS. His research interests include analog and RFIC design.



SHOBA KRISHNAN (Member IEEE) received the B.Tech. degree from Jawaharlal Nehru Technological University, India, in 1987, and the M.S. and Ph.D. degrees from Michigan State University, East Lansing, MI, USA, in 1990 and 1993, respectively. From 1995 to 1999, she was with the Mixed-Signal Design Group, LSI Logic Corporation, Milpitas, CA, USA, where she worked on high-speed data communication IC design and testing. She is currently a Professor with the Department of Electrical and Computer Engineering, Santa Clara

University, CA, USA. She has been part of the Electrical Engineering Faculty since 1999. Her expertise and research interests include analog and mixed-signal integrated circuit design and testing with projects in high-speed data communication systems with special emphasis on power, clock and data I/O circuits.



ALLEN A. SWEET (Life Member, IEEE) was born in Providence, RI, USA, on July 5, 1943. He received the B.S. degree in electrical engineering from Worcester Polytechnic Institute, Worcester, MA, USA, in 1966, and the M.S. and Ph.D. degrees in electrical engineering from Cornell University, Ithaca, NY, USA, in 1968 and 1970, respectively. He has been involved in microwave design and consulting service since 1976 and has been an Adjunct Professor with the Department of Electrical and Computer Engineering, Santa Clara University, Santa Clara, CA, USA, since 2002. He is currently the Vice President and Director of the Nano technology division of Vida Products Rohnert Park, CA, USA. He is the author of five books, two published by Artech House, Boston, MA, USA, and three published by IUniverse Publications in Bloomington, IN, USA. His research interests include the area of the nano technology of garnet crystals, and in developing methods for understanding the design of low phase noise oscillators. Dr. Sweet was the co-recipient of the 1977 IEEE MTT microwave prize.

University, Santa Clara, CA, USA, since 2002. He is currently the Vice President and Director of the Nano technology division of Vida Products Rohnert Park, CA, USA. He is the author of five books, two published by Artech House, Boston, MA, USA, and three published by IUniverse Publications in Bloomington, IN, USA. His research interests include the area of the nano technology of garnet crystals, and in developing methods for understanding the design of low phase noise oscillators. Dr. Sweet was the co-recipient of the 1977 IEEE MTT microwave prize.